The American Journal of Pathology, Vol. 173, No. 5, November 2008

DOI: 10.2353/ajpath.2008.080483

Immunopathology and Infectious Diseases

Interaction of the Lyme Disease Spirochete *Borrelia burgdorferi* with Brain Parenchyma Elicits Inflammatory Mediators from Glial Cells as Well as Glial and Neuronal Apoptosis

Geeta Ramesh,* Juan T. Borda,† Jason Dufour,‡ Deepak Kaushal,* Ramesh Ramamoorthy,* Andrew A. Lackner,† and Mario T. Philipp*

From the Divisions of Bacteriology and Parasitology, Comparative Pathology,† and Veterinary Medicine,‡ Tulane National Primate Research Center, Tulane University, Covington, Louisiana*

Lyme neuroborreliosis, caused by the spirochete *Borrelia burgdorferi*, often manifests by causing neurocognitive deficits. As a possible mechanism for Lyme neuroborreliosis, we hypothesized that *B. burgdorferi* induces the production of inflammatory mediators in the central nervous system with concomitant neuronal and/or glial apoptosis. To test our hypothesis, we constructed an *ex vivo* model that consisted of freshly collected slices from brain cortex of a rhesus macaque and allowed live *B. burgdorferi* to penetrate the tissue. Numerous transcripts of genes that regulate inflammation as well as oligodendrocyte and neuronal apoptosis were significantly altered as assessed by DNA microarray analysis. Transcription level increases of 7.43-fold ($P = 0.005$) for the cytokine tumor necrosis factor-α and 2.31-fold ($P = 0.016$) for the chemokine interleukin (IL)-8 were also detected by real-time-polymerase chain reaction array analysis. The immune mediators IL-6, IL-8, IL-1β, COX-2, and CXCL13 were visualized in glial cells *in situ* by immunofluorescence staining and confocal microscopy. Concomitantly, significant proportions of both oligodendrocytes and neurons undergoing apoptosis were present in spirochete-stimulated tissues. IL-6 production by astrocytes in addition to oligodendrocyte apoptosis were also detected, albeit at lower levels, in rhesus macaques that had received *in vivo* intraparenchymal stereotaxic inoculations of live *B. burgdorferi*. These results provide proof of concept for our hypothesis that *B. burgdorferi* produces inflammatory mediators in the central nervous system, accompanied by glial and neuronal apoptosis. *(Am J Pathol 2008, 173:1415–1427; DOI: 10.2353/ajpath.2008.080483)*

Lyme disease is a tick-borne infection caused by the spirochete *Borrelia burgdorferi* (sensu lato).[1,2] The remarkable organ pleiotropism of this spirochete results in diverse disease manifestations such as acute or chronic arthritis, myocarditis, and neuroborreliosis.[3] Lyme neuroborreliosis affects 15 to 25% of patients with erythema migrans, the red skin-rash that in humans signals the point of entry of *B. burgdorferi*, and may involve both the peripheral and central nervous systems (CNS).

Neuroborreliosis may manifest early, within the first few weeks to months of the appearance of erythema migrans, as a meningitis, often as part of the Garin-Bujadoux-Bannwarth syndrome, or, more seriously, as encephalomyelitis. The latter is less common than the meningitis but shares with it the presence of lymphocytic pleocytosis in the cerebrospinal fluid (CSF) and intrathecal anti-*B. burgdorferi* antibody production. This disorder's importance is derived from the fact that it can lead to irreversible CNS damage,[4] of the type that may be attributed to neuronal loss. Later in the course of disease, several months after infection, encephalopathies may appear. Patients with this late symptom complain of specific memory and/or intellectual impairment, often associated with incapacitating fatigue.[4] Brain lesions from Lyme neuroborreliosis patients show vasculitis and subarachnoid hemorrhage[5–8] as well as multifocal encephalitis with

Supported by the National Institutes of Health (grants NS048952, RR00164, G20 R018397-01, and G20 R019607-01) and the Centers for Disease Control and Prevention (grant UO1-CI000153).

Accepted for publication August 5, 2008.

Supplemental material for this article can be found on *http://ajp.amjpathol.org*.

Address reprint requests to Mario T. Philipp, Division of Bacteriology and Parasitology, Tulane National Primate Research Center, Tulane University, 18703 Three Rivers Rd., Covington, LA 70433. E-mail: philipp@tulane.edu.

large areas of demyelination in perivascular white matter, at times associated with the presence of *B. burgdorferi* DNA.[9–12] Neurological disturbance limited to the spinal cord can manifest clinically as acute transverse myelitis and leptomeningitis.[9,12]

Cytokines and chemokines are key mediators in various kinds of inflammatory neurodegenerative diseases and play an important role in promoting CNS injury.[13–16] Various cytokines such as interleukin (IL)-1β, IL-6, tumor necrosis factor (TNF)-α, interferon-γ, and transforming growth factor-β have been detected in the CSF of Lyme neuroborreliosis patients, indicating that they play a role in the pathogenesis of this form of Lyme disease.[17–20] Several chemokines also have been found in the CSF of such patients, including the B-lymphocyte chemokine CXCL13 (BLC),[21] interleukin 8, CXCL8 (IL-8), macrophage inflammatory proteins, CCL3 (MIP-1α) and CCL4 (MIP-1β),[22] interferon-inducible T-cell chemoattractant, CXCL11 (I-TAC), and monocyte chemotactic protein CCL2 (MCP-1).[23] Soluble intercellular adhesion molecule-1, ICAM-1 (CD64), also has been observed.[24]

Lyme disease signs and disease progression in the rhesus macaque are similar to those of human Lyme disease, which makes the use of this model both appropriate and valuable.[25–32] Observations from human Lyme neuroborreliosis patients as well as studies in rhesus monkeys suggest that inflammation plays an important role in disease pathogenesis. We therefore hypothesized that *B. burgdorferi* spirochetes cause inflammation in the CNS by inducing cytokines, chemokines, and other immune mediators in glial cells. In this inflammatory milieu, both glial and neuronal function as well as survival could be affected, contributing eventually to cell death by apoptosis.

To test our hypothesis we set up an experimental design aimed at facilitating the direct interaction of live *B. burgdorferi* with brain parenchyma of rhesus monkeys. For our *ex vivo* model we obtained fresh brain slices from the frontal cortex of rhesus monkeys because this area is known to control both motor and memory functions,[33] and exposed them to live *B. burgdorferi*. The spirochetes readily penetrated the tissue. Brain slices that were incubated with spirochetes or medium alone were surveyed with rhesus-specific DNA microarrays. The up-regulation of genes encoding pro-inflammatory mediators or involved in apoptosis was specifically evaluated. A polymerase chain reaction (PCR) array for common human cytokines and chemokines also was used to confirm the results of the microarrays. We then identified the cells producing selected immune mediators *in situ* by multilabel confocal microscopy and also determined the glial cell types undergoing apoptosis *in situ*. Further, we extended our study into an *in vivo* model in which live spirochetes were injected stereotaxically into rhesus monkey brain parenchyma. The results of these experiments document that live *B. burgdorferi* have the potential to induce immune mediators in glial cells, with concomitant apoptosis of both oligodendrocytes and neurons.

Materials and Methods

Ex Vivo *Experiments*

Animal Information

Brain tissues for *ex vivo* experiments were collected from five rhesus macaques (*Macaca mulatta*) of Indian origin EI55 (female; age, 1.85 years), A434 (female; age, 24.46 years), CL15 (female; age, 3.65 years), FI42 (male; age, 1.88 years), and DN55 (male; age, 6.00 years). These animals were uninfected with *B. burgdorferi* and were slated for euthanasia because they suffered from chronic idiopathic diarrhea. Animals were euthanized by a method consistent with the recommendations of the American Veterinary Medical Association's Panel on Euthanasia.

Incubation of Brain Slices with Live Spirochetes

Fresh brain tissue was obtained from the frontal cortex immediately after euthanasia in phosphate-buffered saline (PBS), pH 7.2 (Invitrogen, Grand Island, NY), at room temperature. The tissue was sliced into 2-mm sections using a brain tissue slicer (Ted Pella Inc., Redding, CA) and tissue slicing blades (Thomas Scientific, Swedesboro, NJ). The slices were placed in separate wells of 12-well plates (Fisher Scientific, Fair Lawn, NJ), each containing 2 ml of RPMI 1640 medium (BioWhittaker, Walkersville, MD), supplemented with 10% fetal bovine serum (Invitrogen). *B. burgdorferi* strain B31 clone 5A19 spirochetes, passage 1 to 3 were grown in Barbour-Stoenner-Kelly medium, supplemented with 6% rabbit serum (Sigma, St. Louis, MO) to late logarithmic phase under microaerophilic conditions. Spirochetes were pelleted at 2000 $\times$ *g* for 30 minutes at room temperature. At the end of the run the rotor was left to coast without breaking so as to minimize damage to the live spirochetes. The culture was washed twice using PBS and resuspended in complete RPMI. Control slices were held in medium alone. Some wells received spirochetes at a final concentration of 1.0×10^7/ml in the presence or absence of brefeldin A (Molecular Probes, Eugene, OR), a fungal metabolite that blocks protein transport[34] at a final concentration of 10 μg/ml. Corresponding control slices were also held in medium plus brefeldin A without spirochetes. The dose of spirochetes was arrived at by incubating brain slices in the presence of brefeldin A with spirochete concentrations of 1.3, 1.7, 2.5, 5.0, and 10.0×10^6/ml, to cover a wide range of inoculum sizes. Optimal production of inflammatory mediators was observed at the highest spirochetal concentration, which was therefore chosen for all of the *ex vivo* experiments. The brain slices were then incubated at 37°C for 4 or 8 hours in a humidified 5% CO_2 incubator. These time points were selected based on viability results obtained in preliminary experiments that were done by incubating 2-mm brain slices in medium alone or medium containing 10 μg/ml of befeldin A for various time intervals, namely 2, 4, 6, 8, 12, and 24 hours. Cell viability was ascertained from five tissue slices of 16 μm thickness made from each block of

tissue after fixation using 2% paraformaldehyde and cryopreservation as described below, using the terminal deoxynucleotidyl transferase-mediated UTP nick-end labeling (TUNEL)-ApopTagPlus fluorescein *in situ* apoptosis assay (Chemicon, Temecula, CA) as per the manufacturer's instructions. No cell death was seen until 6 hours of incubation in either medium alone or medium containing brefeldin A. Cell death in control slices began to be visible at 8 hours, and dramatically increased after 12 hours and 24 hours of incubation. Thus brain slices that were used for RNA analysis as well as intracytoplasmic cytokine staining described below were incubated for 4 hours, while apoptosis was quantified as described below for both the 4-hour and 8-hour time points. Brain slices that were incubated with spirochetes alone as well as corresponding control slices held in medium alone were used for RNA analysis as well as for the detection of apoptosis *in situ*. Brain slices held in medium containing brefeldin A were used for the detection of intracytoplasmic immune mediators *in situ*. A total of two tissue slices per animal was subjected to each of the conditions described. A total of 10 cryosections was evaluated per tissue slice from animals EI55, A434, CL15, and FI42. The detection of immune mediators as well as apoptosis were qualitatively evaluated in these animals.

Extraction of Total RNA from Tissues

After stimulation, total RNA was extracted from duplicate tissue slices from three animals (EI55, FI42, and DN55) using the RNeasy lipid tissue mini kit designed for tissues such as brain, following the recommendations of the manufacturer (Qiagen Inc., Valencia, CA). Possible DNA contamination was removed by subjecting the RNA to DNase treatment (DNA-free kit; Ambion, Austin, TX). Approximately 1 to 2 μg of each RNA sample was electrophoresed through a 1% agarose-0.1% sarkosyl gel to verify the quality of the preparations.[35] The nucleic acid concentration and purity of the preparations was monitored using a NanoDrop ND-1000 (V3.1) full-spectrum UV/Vis spectrophotometer (NanoDrop Technology Inc., Wilmington, DE). RNA prepared from animal DN55 was stocked as a backup.

Microarray Analysis

Total RNA extracted from two distinct brain slices from one animal (FI42) exposed to spirochetes or medium alone for 4 hours was used in this study. A quantity of 100 ng of total RNA was used to generate Cy-labeled cDNA samples using the a low RNA input linear amplification kit (LRILAK) (Agilent Technologies, Inc., Foster City, CA). Control samples were labeled with Cy3, whereas experimental samples were labeled with Cy5. Labeled cDNA was hybridized overnight to a 44,000-element 60-mer oligonucleotide-based rhesus monkey microarray printed in a 4 $\times$ 44 k format (Agilent Technologies Inc.), which can interrogate the transcription of more than 18,000 unique macaque genes at once. Hybridization was performed in a SciGene 4000 HybOven (SciGene Corp., Sunnyvale, CA) at 65°C for 18 hours, in a rotary chamber at 10 rpm. The slides were then washed using the manufacturer's protocol (Agilent Technologies, Inc.) and scanned in a dual-confocal continuous microarray scanner (GenePix 4000B: Molecular Devices, Sunnyvale, CA), using GenePix Pro version 6.1 as the image acquisition and extraction software. Microarray data were based on duplicate measurements made from two RNA samples extracted from the two frontal cortex tissue slices.

The resulting text data were imported into Spotfire DecisionSite for Functional Genomics (Spotfire Inc., Somerville, MA), filtered, and subjected to statistical analysis.[36] Genes whose expression changed by at least 1.6-fold or more for up-regulated genes and -1.6-fold or less for down-regulated genes (with a corrected one-way analysis of variance, $P < 0.05$) were considered to be differentially expressed in a statistically significant manner. Pathway analysis was performed by uploading significant dataset(s) into Ingenuity Pathways Analysis algorithm (Ingenuity Systems, Redwood City, CA). Only those pathways that were perturbed in a statistically significant manner ($P < 0.05$) were included in the analysis.

Real Time-PCR Array Analysis

Total RNA extracted from two distinct brain slices from two animals (EI55, FI42) exposed to spirochetes or medium alone for 4 hours was used in this study. The RT^{2}ProfilerPCR array APH-021 Human Common Cytokines (SuperArray Bioscience Corp., Frederick, MD) was used according to the manufacturer's instructions to detect the transcripts of common cytokine genes in the RNA samples. PCR amplification was performed with an Applied Biosystems ABI 7700 real-time PCR machine (Applied Biosystems, Foster City, CA) using the appropriate program described in the instructions manual of the RT^{2}ProfilerPCR array kit. The data were analyzed using the SuperArray (now SABiosciences, Frederick, MD) PCR Array Data Analysis software at (*http://www.sabiosciences.com/pcr/arrayanalysis.php*). Data were based on duplicate measurements made from RNA samples extracted from two distinct frontal cortex tissue slices obtained from each of the two animals.

Immunofluorescence Staining for the Detection of Intracytoplasmic Immune Mediators

For *in situ* analysis, tissues were fixed in 2% paraformaldehyde in PBS, pH 7.0 (USB, Cleveland, OH), cryopreserved, and cryosectioned into 16-μm sections as previously described.[37] Brain slices incubated with *B. burgdorferi* plus brefeldin A as well as corresponding control slices held in medium plus brefeldin A were subjected to immunofluorescence staining as previously described.[37] The primary antibodies against various immune mediators, *B. burgdorferi*, as well as phenotypic markers of cells used in this study are listed in Table 1. Relevant isotype controls (Sigma) at the concentration of their respective primary antibodies were also included. All primary antibodies at the appropriate concentrations

Table 1. Primary Antibody and Antibody/Fluorochrome Conjugates against Various Immune Mediators, *B. burgdorferi*, and Phenotypic Markers of Cells

Mediator/cell type	Primary Ab	Isotype	Dilution/ concentration	Source
IL-1β	Anti-human IL-1β	Rabbit IgG	20 μg/ml	RDI, Flanders, NJ
IL-6	Anti-human IL-6	Mouse IgG_{2a}	5 μg/ml	Chemicon, Temecula, CA
IL-8	Anti-human IL-8	Rabbit IgG	10 μg/ml	RDI
TNF-α	Anti-human TNF-α	Mouse IgG_1	20 μg/ml	BD Pharmingen, San Diego, CA
	Anti-rhesus macaque TNF-α	Rat IgG_1	20 μg/ml	R&D Systems, Minneapolis, MN
CXCL13	Anti-human CXCL13	Goat IgG	5 μg/ml	R&D
COX-2	Anti-human COX-2	Rabbit IgG	10 μg/ml	Chemicon
Activated caspase-3	Anti-human Active caspase-3 Ab clone 13847	Rabbit IgG	5 μg/ml	Abcam, Inc. Cambridge, MA
Astrocyte	Anti-human GFAP-cy3	Mouse IgG_1	1:200	Sigma, St Louis, MO
	Anti-human GFAP	Mouse IgG_1	1:200	Sigma
Microglia	Anti-Iba1 synthetic	Rabbit IgG	1:100	Wako Pure Chemicals, Richmond, VA
Oligodendrocyte	Anti-human S-100	Rabbit IgG	1:500	Sigma
	Anti-human MAB 328	Mouse IgM	1:200	Chemicon
Neuron	Anti-mouse NeuN	Mouse IgG_1	1:20	Chemicon
B. burgdorferi	Anti-whole cell preparation	Rabbit IgG	1:250	Accurate Chemicals, Westbury, NY
	Anti-Bb-FITC	Goat	1:10	Kirkegaard and Perry, Gaithersburg, MD

were left on the slides for 1 hour at room temperature, in a humidifying chamber. The slides were then washed with PBS-FT buffer (PBS, pH 7.4, containing 0.2% fish skin gelatin (Sigma) and 0.02% Triton X-100 (MP Biomedicals, Solon, OH) and then held in this buffer for 5 minutes, followed by a rinse with PBS-F buffer (PBS containing 0.2% fish skin gelatin).

The relevant secondary antibodies (either goat anti-mouse, goat anti-rabbit, or goat anti-rat) (Molecular Probes) at a dilution of 1:1000 in PBS, 10% normal goat serum, 0.2% FSG, and 0.02% sodium azide were applied to the tissues and left in the humidified dark slide chamber at room temperature for 30 to 45 minutes. In some cases the Zenon rabbit IgG labeling kit was used (Molecular Probes). Secondary antibodies were conjugated to one of the Alexa fluorochromes, Alexa 488 (green), Alexa 568 (red), or Alexa 633 (blue) (Molecular Probes). Slides were washed and rinsed as described above and then mounted in anti-quenching medium (Sigma). The stained and mounted slides were stored in the dark at 4°C until they were viewed.

The labeling scheme for double and triple labels was as follows. First, primary antibodies to various cytokines were applied to the slides followed by their corresponding secondary antibodies. This was followed by antibodies against specific brain cells, and finally by antibodies against *B. burgdorferi*. Channel 1 was used for visualizing unlabeled primary antibodies to various cytokines or brain cell markers that were bound with secondary antibodies conjugated with Alexa 488, or for visualizing spirochetes when these were stained with fluorescein isothiocyanate-conjugated antibody against *B. burgdorferi*. Channel 2 was used to visualize primary antibodies to various cytokines or cell markers whose respective secondary antibodies were conjugated to Alexa 568 or for primary antibodies conjugated directly to cy3 (red) in the case of GFAP. Channel 3 was used to visualize primary antibody against cytokines or *B. burgdorferi* that had secondary antibodies conjugated to Alexa 633 (Alexa 633 fluoresces in the far red channel but the color is changed to blue at the time of data acquisition on the confocal microscope). The individual antibody-fluorochrome combinations are specified in the respective figure legends.

Cell Types Undergoing Apoptosis

Tissues exposed to live spirochetes for 4 and 8 hours as well as corresponding control tissues held in medium alone for the same time were used for the evaluation of apoptosis. Sections were stained for any one of the following brain cell markers NeuN (neurons), IBA-1 (microglia), GFAP-cy3 (astrocytes), or S-100 (astrocytes and oligodendrocytes) by immunofluorescence staining followed by secondary antibodies conjugated with Alexa Flour 568 as described above. Sections were fixed in 2% paraformaldehyde for 15 minutes, followed by a 15-minute wash in PBS. Sections were then subjected to the TUNEL-ApopTagPlus fluorescein *in situ* apoptosis assay (Chemicon) as per the manufacturer's instructions. Sections were also stained with anti-*B. burgdorferi* antibody as described above followed by secondary antibody conjugated to Alexa Fluor 633. To confirm the identity of S-100-staining cells as oligodendrocyte, S-100-stained (Alexa Fluor 568) sections were also stained with anti-GFAP followed by secondary antibody conjugated to Alexa Fluor 633 (blue), before doing the TUNEL assay because astrocytes are also known to express S-100.[38] Cells that were only positive for S-100 (labeled red) were

regarded as oligodendrocytes, whereas those that were labeled pink because of an overlap of S-100 (red) and GFAP (blue) were considered to be astrocytes. Anti-MAB 328, which is specific for oligodendrocytes and does not label astrocytes, was used as well, but S-100 staining was used for counting apoptotic oligodendrocytes because it proved better for delineating discrete oligodendrocytes. Anti-mAb 328 also stained myelin, resulting in large patches of myelin-stained areas making it unsuitable for counting single cells. Slides were washed and mounted as described above and stored at 4°C in the dark until viewed. Apoptotic cells from 10 fields (more than 500 cells in all cases) were counted from each section for the various incubation conditions and for the 4- and 8-hour time points, respectively. All counts were made by viewing slides under a fixed magnification of ×63 (corresponding to an area of 0.05 mm^2) using the confocal microscope (see below).

Activated Caspase-3 Assay

Immunofluorescence staining for activated caspase-3 was done on sections that were serial sections to those showing cell death by the TUNEL assay. For this, sections stained previously for brain cell markers as described above were stained with a rabbit polyclonal anti-active-caspase-3 primary antibody, clone ab13847 (Abcam Inc., Cambridge, MA) at a concentration of 5 μg/ml, followed by goat anti-rabbit IgG Alexa Fluor 488 as the secondary antibody.

Confocal Microscopy

Confocal microscopy was performed using a Leica TCS SP2 confocal microscope equipped with three lasers (Leica Microsystems, Exton, PA). Differential interference contrast imaging for the observation of nonlabeled tissue during fluorescent confocal image collection was also used. Images of individual channels were merged to obtain images containing all channels. An average of 20 optical sections of 0.8 μm in thickness were examined for each tissue slice that was 16 μm in thickness at a resolution of 512 × 512 pixels. The × 63 objective that was used in this study has a working distance of 70 μm. Thus the entire thickness of the 16-μm tissue slices was effectively scanned. Further, as mentioned, 10 fields were viewed per section. NIH Image (*http://rsb.info.nih.gov/nih-image/*; National Institutes of Health, Bethesda, MD) and Photoshop CS3 (Adobe Systems Inc., San Jose, CA) were used to assign colors to each fluorochrome and the differential contrast image (gray scale).

In vivo *Experiments*

Stereotaxic Inoculation of Live B. burgdorferi into Brain Parenchyma

Four rhesus macaques of Chinese origin CB64 (male; age, 5.90 years), CV57 (male; age, 6.39 years), BV64 (male; age, 7.42 years), and CM60 (male; age, 6.19 years) were used for this experiment. The protocol was approved by the Institutional Animal Care and Use Committee of the Tulane National Primate Research Center, and the procedure used for euthanasia was consistent with the recommendations of the American Veterinary Medical Association's Panel on Euthanasia.

B. burgdorferi was grown to late logarithmic phase as described above. On the day of inoculation, spirochetes were spun down gently and washed twice with endotoxin-free saline (Hospira, Inc., Lake Forest, IL) as described and resuspended to the desired count (1×10^6/ml). Normal rhesus macaques were subjected to magnetic resonance imaging of the brain a week before inoculation to monitor the normal status of the brain as well as for locating reference points to help with identifying the actual coordinates to be used for the stereotaxic inoculations. Physical examinations, the results of which were normal, were also done at the time of magnetic resonance imaging and before inoculation. A total of 15 μl of the above bacterial suspension of live spirochetes was stereotaxically inoculated into the right side of the brain after routine surgical procedures as follows. The first site (A) was situated 5.7 mm lateral from the mid line at the level of the optic chiasma, the second (B) was 10 mm caudal to the first at the level of the caudate nucleus, and the third site (C) was 32 mm caudal to the first site. The inoculations were made at two levels at each site, distributing 2.5 μl of bacterial suspension into the gray matter and 2.5 μl into the white matter (a total of 5000 spirochetes per site). Inoculations on the left side of the brain (sham) mirrored the position of those on the right side, and consisted of the same volumes of endotoxin-free saline but without spirochetes (sites D, E, and F). Two animals (CB64, CV57) received a dose of 5000 spirochetes per site whereas the other two (CM60, BV64) received 50,000 spirochetes per site. One animal from each set was euthanized 2 weeks after inoculation (CV57 and CM60) whereas the other two were euthanized 1 month after inoculation (CB64 and BV64). Brain tissue from the sites of inoculation (A, B, and C) as well as from the control side (D, E, and F), were obtained at necropsy immediately after euthanasia. Tissue was transported in PBS at room temperature, and immediately processed for stimulation of intracytoplasmic cytokines as described earlier.[37] Tissues were also fixed directly in 2% paraformaldehyde as described above and used for the analysis of apoptotic cells by the *in situ* TUNEL assay as described above.

Statistical Analysis

The statistical significance of the apoptosis data was evaluated using the one-way analysis of variance nonparametric analysis, followed by the Tukey's stringency test using PRISM software (IBM, Armonk NY). A corrected one-way analysis of variance was used to analyze the microarray data using Spotfire software (Spotfire DecisionSite for Functional Genomics, Spotfire Inc.). Statistical analysis of the PCR array data was done using the

SuperArray (now SABiosciences) PCR Array Data Analysis software.

Results

Rhesus Monkey DNA Microarray Analyses and PCR Human Array Analyses of Genes that Regulate Immune Function

A global overview of the response mounted by brain cells against spirochetes as revealed by our rhesus microarray analyses suggests that spirochetes elicited an inflammatory milieu in brain slices. A large number of genes that regulate the immune response in the CNS were perturbed (Supplemental Table 1, *http://ajp.amjpathol.org*). The National Center for Biotechnology Information (NCBI) identification number, the fold change, as well as the reported functions of the gene transcripts that were perturbed are listed. Two genes were up-regulated more than a 100-fold, the chemokine (C-C motif)-like member A1 (FAM19A1), which belongs to a family of brain-specific chemokines that act as regulators of immune and nervous cells. This gene was up-regulated by 491-fold (NCBI NM_213609). In addition, the natural-killer cell receptor (KIR2DL3) was up-regulated by 140-fold (NCBI NM_014511). Genes that were up-regulated between 10- and 100-fold were corticotrophin-releasing hormone (NCBI NM_000756; 44.6-fold), which plays a key role in immune modulation in the nervous system via the hypothalamus pituitary adrenal axis, the pyrimidinergic receptor P2Y, G-protein coupled 6 (NCBI NM_004154; 26.9-fold), which is involved in microglial immune activation, induction of the chemokine IL-8, and mitogen-activated protein kinase p38, and has important immunomodulatory roles in the CNS; importantly, the pro-inflammatory cytokine TNF-α transcript also was up-regulated (NCBI NM_000594; 21.7-fold). Finally, several immune response-related genes were significantly up-regulated less than 10-fold, including the signal transducer and activator of transcription 3 (STAT3, NCBI NM_213662; 7.23-fold). This key transcription factor, which regulates the activation and function of IL-6, IL-8, as well as COX-2, also plays a key role in many cellular processes such as growth and apoptosis. The transcripts of various other genes such as chemokines and transcription factors that affect the immune response mounted by the brain were also up-regulated (Supplemental Table 1, *http://ajp.amjpathol.org*).

In addition, real-time PCR human array analysis for common cytokines showed a mean positive fold increase of 7.43 ($P = 0.005$) for the cytokine TNF-α and 2.31 ($P = 0.016$) for the chemokine IL-8 in the tissues stimulated with live spirochetes for 4 hours as compared to that seen in tissue held in medium alone. This result validates the fold increase of TNF-α transcript that we observed in the rhesus microarray analysis. Collectively, these data support our hypothesis that spirochetes can elicit an inflammatory environment on penetration of the brain parenchyma.

Assessment of the Production of Inflammatory Mediators in Glial Cells by Confocal Microscopy

To further confirm the microarray and PCR data and to examine the relationship between the presence of *B. burgdorferi* and cytokines produced by various cell types, we examined brain sections for the detection of immune mediators in glial cells by immunofluorescence staining and confocal microscopy. We focused our attention on IL-6, IL-1β, TNF-α, IL-8, and CXCL13 because these mediators have been reported to play a role in the acute stages of Lyme neuroborreliosis in humans.[17–21] We also looked for the presence of the immune mediator COX-2 because it is known to be involved in both inflammation and apoptosis in brain disorders.[39] Intracytoplasmic staining for cytokines in tissue sections stimulated with live spirochetes in the presence of brefeldin A showed presence of IL-6 in astrocytes (Figure 1A). Cells other than astrocytes also produced IL-6, as evidenced by the IL-6-specific staining of other areas of the tissue section. The highest amount of IL-6 was found along the section's edge, where most of the spirochetes congregated. No signal for IL-6 was detected in control tissue slices held in medium containing brefeldin A alone for 4 hours (Figure 1B). IL-1β (in red) was produced by microglia (Figure 1D). No signal for IL-1β was detected in control tissue slices held in medium containing brefeldin A alone for 4 hours (Figure 1E).

We extended the observations made in our *ex vivo* model into an *in vivo* setting by stereotaxically inoculating live spirochetes into the brain parenchyma of rhesus macaques, as described in Materials and Methods. Immunofluorescence staining and confocal microscopic evaluation of brain tissue slices obtained at postmortem from these animals and processed for intracytoplasmic cytokine detection showed presence of IL-6 in astrocytes in the three sites inoculated with live spirochetes but not in sections processed from the corresponding control sites that received only saline (not shown). A representative image from one animal showing the co-localization of IL-6 and the astrocyte marker (GFAP) is shown in Figure 1C. The presence of traces of spirochetal antigen in the vicinity of the astrocyte can be seen in blue. Intact spirochetes were not detected in any of the inoculation sites.

The chemokine IL-8 localized both to astrocytes and microglia (Figure 2, A and B, respectively). A positive signal for IL-8 was also found in cells other than astrocytes and microglia, possibly endothelial cells lining blood vessels (Figure 2B). The B-cell-attracting chemokine CXCL13 was also detected in microglia in spirochete-stimulated tissues (Figure 2C). The immune mediator COX-2 was detected in both astrocytes (Figure 2D) and microglia (Figure 2E). None of the pro-inflammatory mediators described above was detected in brain slices that were incubated for 4 hours in medium that contained only brefeldin A (not shown). These data strongly support our hypothesis that glial cells elicit in the CNS an inflammatory milieu in response to *B. burgdorferi*.

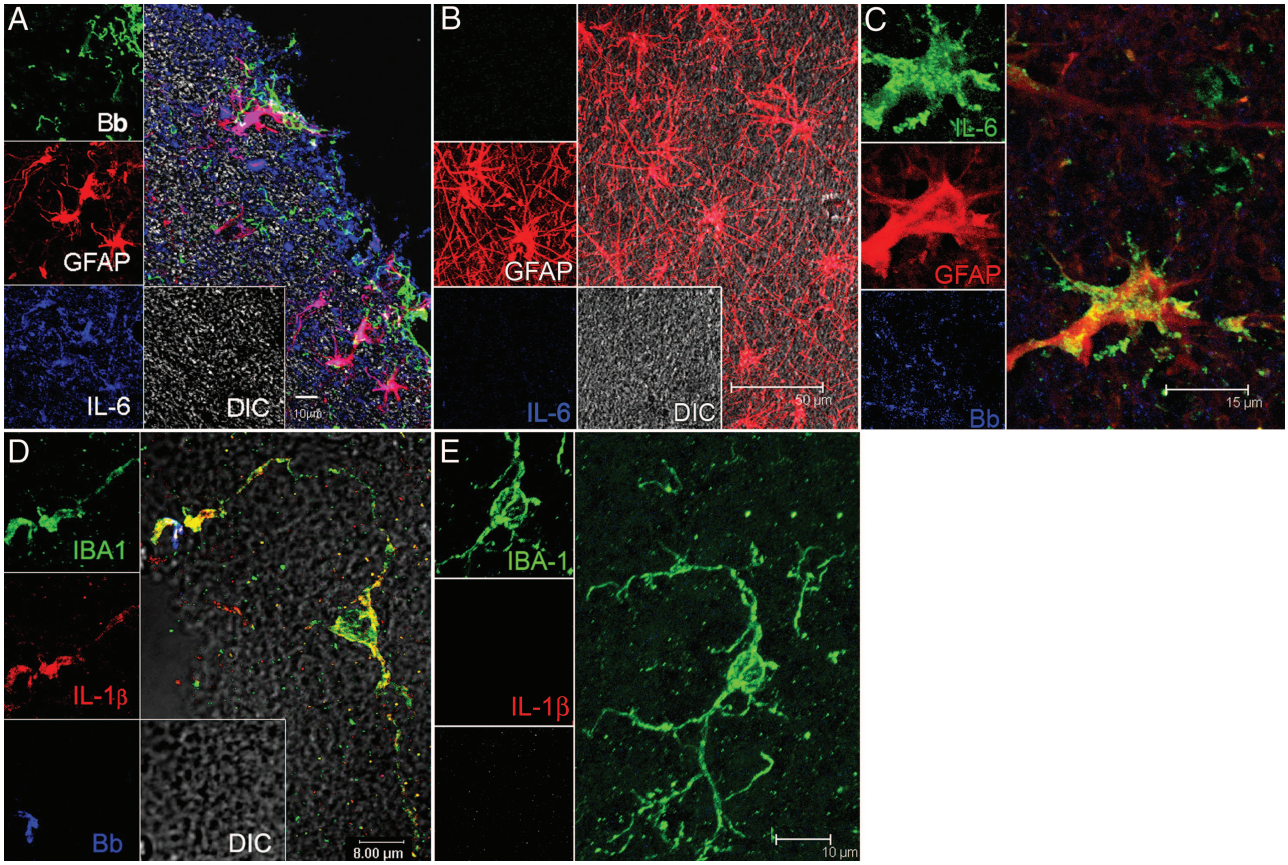

Figure 1. Visualization of the production of cytokines IL-6 and IL-1β by glial cells in *B. burgdorferi*-exposed frontal cortex tissue explants and brain sections from animals given stereotaxic inoculations with *B. burgdorferi*. **A:** IL-6-producing astrocytes appear pink because of co-localization of IL-6 antibody (labeled blue) with antibody to the astrocyte marker GFAP (red). The spirochetes stained with fluorescein isothiocyanate-labeled *B. burgdorferi* antibody (Bb) appear green. Unstained tissue appears gray under differential interference contrast (DIC). **B:** Astrocytes labeled with GFAP (red) in brain tissue slices incubated in medium plus brefeldin A in the absence of spirochetes had no detectable IL-6. **C:** Visualization of IL-6-producing astrocytes in a tissue section taken at the site of inoculation from an animal given stereotaxic inoculations with live *B. burgdorferi*. IL-6-producing astrocytes appear yellow because of co-localization of antibody to IL-6 (green) and antibody to the astrocyte marker GFAP (red) in the vicinity of *B. burgdorferi* antigen stained blue. **D:** IL-1β-producing microglia appear yellow because of co-localization of antibody to the microglial marker IBA 1 (green) and antibody to IL-1β (red). Spirochetes in this image appear blue. **E:** Microglia labeled with IBA-1 (green) in brain slices incubated in medium plus brefeldin A in the absence of spirochetes had no detectable IL-1β.

DNA Microarray Survey of Genes Involved in Apoptosis

We hypothesized that mediators elicited by spirochetes could induce apoptosis of both glial cells and neurons. Microarray analysis revealed that more than 30 apoptosis-related gene transcripts were perturbed after exposure of rhesus monkey brain tissue explants to live *B. burgdorferi* for 4 hours. Importantly, many genes that specifically induce apoptosis of oligodendrocytes as well as neurons were strongly up-regulated (Supplemental Table 2, *http://ajp.amjpathol.org*). For example, the transcript of the gene coiled-coil-helix domain-containing six (NCBI NM_032343), which regulates mitochondria-mediated apoptosis was up-regulated 2048-fold. The transcript of the gene Cbp/p300-interacting transactivator, with Glu/Asp-rich carboxy-terminal domain 4 (NCBI NM_133467), which is an oligodendrocyte-specific tumor-repressor that is silenced in oligodendrocyte tumors, was up-regulated 124.49-fold. The transcript of formin homology-2 domain-containing 1 (NCBI NM_013241), which is associated with the caspase-3-mediated apoptosis pathway, was up-regulated 43.40-fold. The transcript of the embryonic lethal, abnormal vision, Drosophila-like 4 gene (NCBI NM_021952), which is associated with inflammation and neuronal death and is up-regulated in Parkinson's disease, was up-regulated in spirochete-stimulated tissues by 9.98-fold. The transcript of neuronal pentraxin 1 (NCBI BX537550), which is involved in synapse loss, neurite damage, and apoptotic neuronal death and is also overexpressed in Alzheimer's brain was up-regulated by 8.39-fold. The transcript of glutamate receptor, ionotropic, delta 2 (NCBI NM_001510), which regulates the functions of glutamate, one of the predominant excitatory neurotransmitters in the mammalian brain that is known to mediate neuronal apoptosis by excitotoxicity, was up-regulated by 4.40-fold. The transcripts of various other genes that affect glial and neuronal survival were also perturbed (Supplemental Table 2, *http://ajp.amjpathol.org*). These data support our notion that the global inflammation induced by *B. burgdorferi* as it enters the brain parenchyma also creates the conditions for apoptosis of glial cells and neurons.

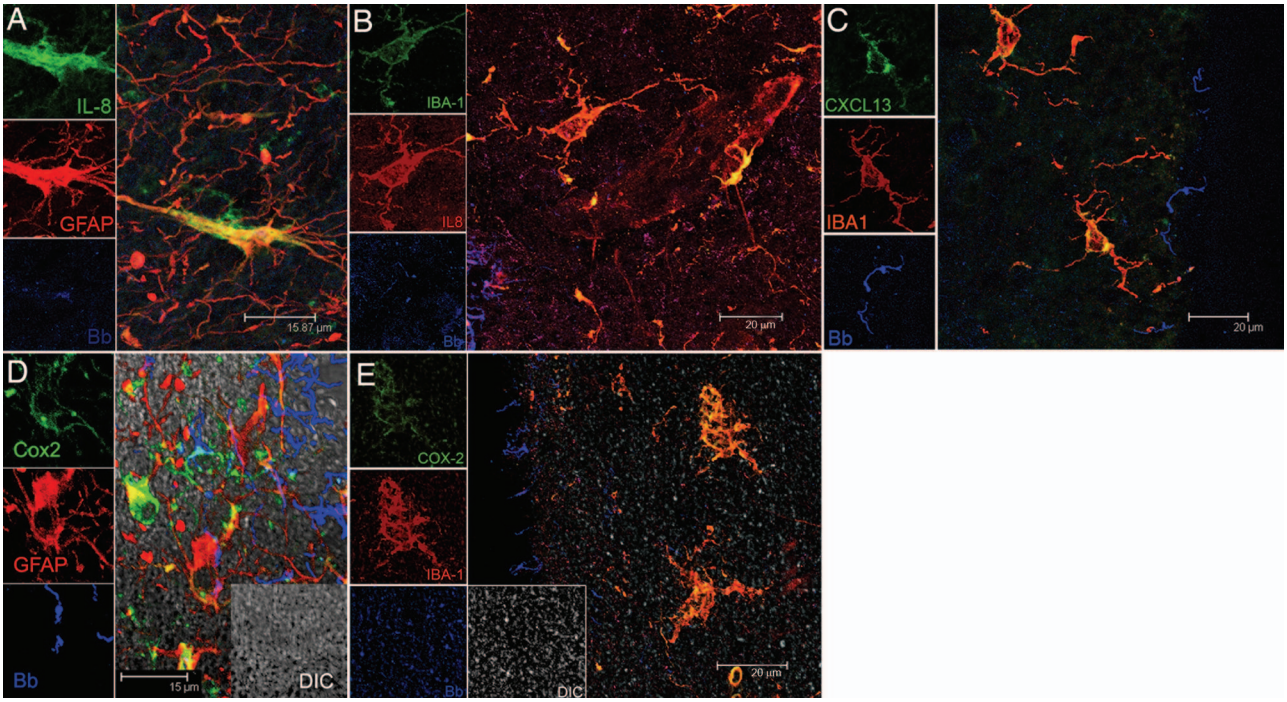

Figure 2. Visualization of the production of IL-8, CXCL13, and COX-2 by glial cells in *B. burgdorferi*-exposed frontal cortex tissue explants. **A:** IL-8-producing astrocytes appear yellow because of co-localization of IL-8 antibody (green) and antibody to astrocyte marker GFAP (red). **B:** IL-8-producing microglia appear yellow because of co-localization of IL-8 antibody (red) and antibody to microglial marker IBA 1 (green). **C:** Production of CXCL13 in microglia appears yellow because of overlap of antibody to CXCL13 (green) and IBA 1(red). **D:** COX-2-producing astrocytes are seen as yellow because of overlap of GFAP-staining astrocytes (red) and COX-2 (green). **E:** COX-2-producing microglia are seen as yellow because of overlap of IBA-1-staining microglia (red) and COX-2 (green). Spirochetes appear blue in all sections.

Qualitative and Quantitative Assessment of Glial and Neuronal Apoptosis

Oligodendrocyte and neuronal apoptosis was assessed *in situ* in brain tissue explants from the four animals used for these studies, as described in Materials and Methods. Apoptosis was detected by both TUNEL and activated caspase-3 assays, visualized as a green signal that co-localized with either oligodendrocytes (stained red only with antibody to S-100) or neurons (stained red with antibody to NeuN). No apoptosis signal was seen in astrocytes or microglia. Because similar qualitative results were obtained in all animals, apoptosis was quantified only in explants from two animals, EI55 and A434. The amount of apoptotic cells seen by the active caspase-3 assay was generally a third of that seen by the TUNEL assay for all slides evaluated. There was a gradient in the number of apoptotic cells seen, with the largest number of apoptotic cells being present at the edge of the brain tissue, which coincided with a higher concentration of spirochetes. A representative image of $S100^{+}$ cells (oligodendrocytes) positive for activated caspase-3 in spirochete-exposed tissues is shown in Figure 3A. The percentage of apoptotic oligodendrocytes after 4 and 8 hours of incubation with live spirochetes in animal EI55 is shown in Figure 3B. Exposure of rhesus brain tissue to live spirochetes for 4 hours resulted in 24.56 ± 6.07%, of oligodendrocytes showing activated caspase-3, which was significant ($P < 0.001$) as compared to control brain tissue from the same animal incubated for 4 hours in medium devoid of spirochetes. Oligodendrocyte apoptosis increased to 27.42 ± 6.12% after 8 hours of exposure to spirochetes. A higher and also significant ($P < 0.001$) proportion of oligodendrocyte cell death was detected by the *in situ* TUNEL assay (Figure 3B) as compared to that seen in respective control tissues held in medium alone for similar periods of time. No apoptosis was detected in tissues held in medium alone for 4 hours, and minimal levels after 8 hours.

Neuronal apoptosis was evaluated in tissue sections adjacent to those that showed oligodendrocyte apoptosis. Neuronal cell death, as evidenced by the activated caspase-3 assay in animal EI55 are shown in Figure 3C. Overall, the level of neuronal apoptosis was lower than that seen in oligodendrocytes (Figure 3D). After 4 hours of co-incubation with *B. burgdorferi*, 1.35 ± 1.35% ($P < 0.05$) of neurons were positive for activated caspase-3, and 3.85 ± 1.66 after 8 hours. As with the oligodendrocytes, higher and significant levels ($P < 0.001$) of neuronal cell death were detected by the TUNEL assay (Figure 3D) as compared to the respective control tissues held in medium alone. Similar results were obtained with brain slices obtained from a second animal A434 (not shown). These data show that spirochetes can induce apoptosis of both oligodendrocytes and neurons in rhesus brain tissue explants. Although direct contact between dying cells and spirochetes was evident in some instances, we speculate that the inflammatory milieu elicited by the organisms must have contributed to glial and neuronal cells death.

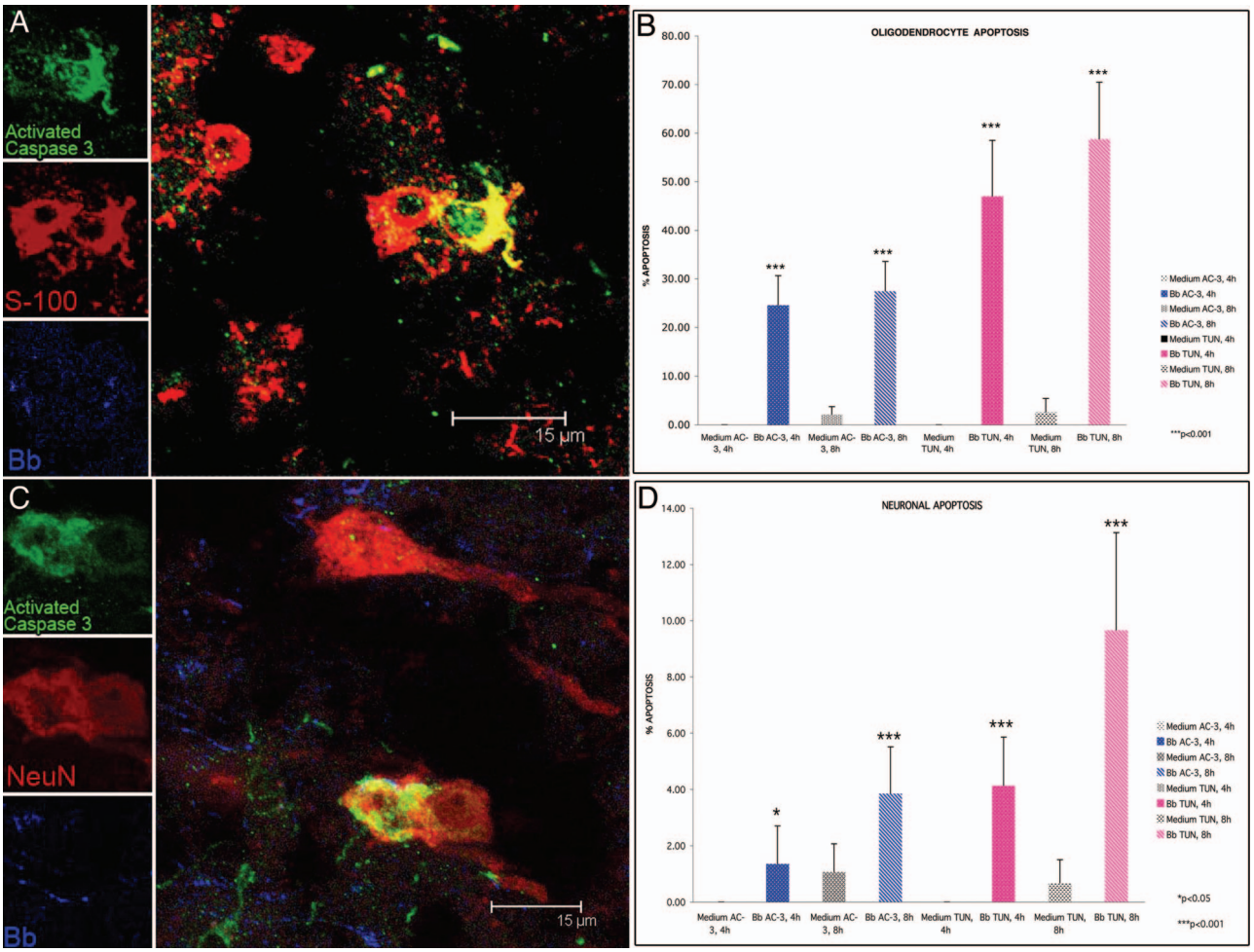

Figure 3. Oligodendrocyte and neuronal apoptosis in frontal cortex brain tissue exposed to live *B. burgdorferi*. **A:** Confocal micrograph showing apoptotic oligodendrocytes as yellow because of co-localization of antibody to active caspase-3 (green) and antibody to S-100 antigen (red). Spirochetes in this section appear blue. **B:** Percentage of oligodendrocytes (S-100-positive, GFAP-negative) undergoing apoptosis after 4 hours and 8 hours of exposure to live *B. burgdorferi* as quantified by both the active caspase-3 (AC-3) and *in situ* TUNEL assays (TUN). **C:** Confocal micrograph showing apoptotic neurons as yellow because of co-localization of antibody to active caspase-3 (green) and antibody to the neuronal marker NeuN (red). Spirochetes appear blue in color. **D:** Percentage of neurons undergoing apoptosis after 4 hours and 8 hours of exposure to live *B. burgdorferi* as quantified by both the active caspase-3 (AC-3) and *in situ* TUNEL assays (TUN).

Apoptosis of oligodendrocytes, as quantified by the *in situ* TUNEL assay, was also observed in our *in vivo* model in which all four animals were stereotaxically inoculated with live *B. burgdorferi*. No apoptosis of astrocytes and microglia was observed. Figure 4A shows a representative image of oligodendrocytes labeled with S-100 showing a positive signal for the TUNEL assay in their nuclei, in the vicinity of *B. burgdorferi* antigen. The maximum levels of oligodendrocyte apoptosis was seen in animal CM60 (Figure 4B), site A: 12.08% ± 6.9, site B: 9.17% ± 4.79, site C: 8.95% ± 4.51), that received the higher dose of 50,000 spirochetes per site and was sacrificed 2 weeks after inoculation. Minimal apoptosis was also seen on the control sites inoculated with saline (Figure 4B). A mean of 7.89% oligodendrocyte apoptosis was seen in animal CV57 that got the lower dose of 5000 spirochetes per site and that was also sacrificed 2 weeks after inoculation. The animals that were sacrificed 1 month after inoculation had a mean percent oligodendrocyte apoptosis of 7.87% (animal CB64, 5000 spirochetes per site) and 6.52% (animal BV64, 50,000 spirochetes per site). Low numbers of TUNEL-positive neurons were also observed in all sites where *B. burgdorferi* had been inoculated, in all of the animals. However, these were not statistically significant as compared to their respective control sites that received only saline, except for site B in animal CB64, which showed a significant difference with respect to the contralateral control site E (1.65% ± 1.07 versus 0.41% ± 0.053, $P < 0.05$).

Discussion

The pathogenesis of Lyme neuroborreliosis is poorly understood. The direct interaction of the spirochete with glial and neuronal cells as well as the host response to the organism may result in neuronal damage. In this study we assessed both *ex vivo* and *in vivo* the responses of brain tissues, by evaluating the expression of pro-inflammatory immune mediators elicited on interaction

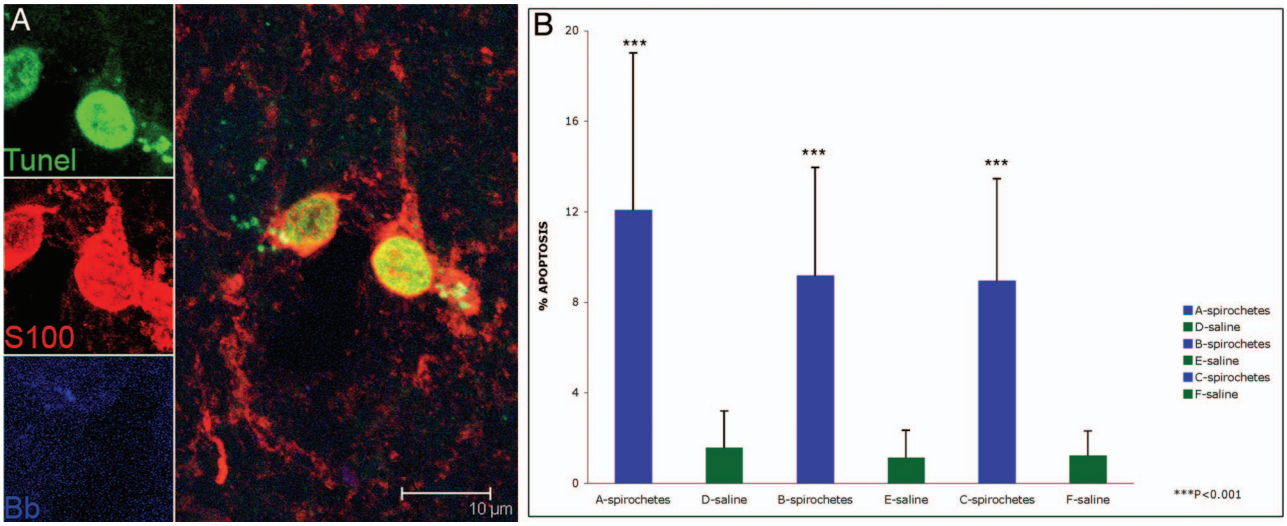

Figure 4. Oligodendrocyte apoptosis observed in rhesus CM60 given stereotaxic inoculations with live *B. burgdorferi*. **A:** Apoptotic oligodendrocytes show TUNEL-positive nuclei stained green. Oligodendrocytes appear red because of staining with antibody to S-100. *B. burgdorferi* antigen appears blue in color. **B:** Percentage of oligodendrocytes (S-100-positive, GFAP-negative) undergoing apoptosis in brain sections from the sites of spirochetal inoculation (**A–C**) and corresponding control sites (**D–F**) as quantified by the *in situ* TUNEL assay.

with live *B. burgdorferi* spirochetes. We also addressed our hypothesis that this inflammatory response to *B. burgdorferi* could contribute to cell death by evaluating the presence of concomitant apoptosis of both glial and neuronal cells. The immune mediators IL-6, IL-8, IL-1β, COX-2, and CXCL13 were visualized in glial cells *in situ* by immunofluorescence staining and confocal microscopy. Concomitantly, a significant proportion of both oligodendrocytes and neurons undergoing apoptosis were present in spirochete-exposed tissues. The observation that the largest number of cells producing immune mediators as well as those undergoing apoptosis coincided with the presence of large number of spirochetes along the edges of the brain tissue suggests, but does not prove, that these phenomena are related. The high number of significantly perturbed transcripts of genes that regulate immune function, as revealed in our microarray analysis of live spirochete-stimulated brain tissues (Supplemental Table 1, *http://ajp.amjpathol.org*), subscribes to the notion that spirochetes can have a powerful effect on the regulation of inflammation in the brain parenchyma. Indeed, transcription factors and immune activators that regulate the synthesis and activation of cytokines and chemokines in the brain were seen to be perturbed as a result of spirochete stimulation (Supplemental Table 1, *http://ajp.amjpathol.org*).

We focused on evaluating the cellular source of the pro-inflammatory cytokines IL-6, IL-1β, and TNF-α, and the chemokines CXCL13 and IL-8 because these mediators have been documented to play a role in acute Lyme neuroborreliosis.[17–19,21,22] IL-6 was produced by numerous cells and cell types in rhesus brain tissue that was incubated with live spirochetes *ex vivo*. Of these we identified the astrocyte as a major glial cell type involved. Importantly, stereotaxic intracerebral inoculation of live spirochetes *in vivo* also resulted in production of IL-6 by astrocytes. IL-6 mRNA has also been shown to be expressed at high levels in the CNS of the rhesus macaques infected with *B. burgdorferi* by others.[40]

Reactive astrogliosis has been shown to be a consequence of increased expression of IL-6 in the brain.[41] Markers of astrogliosis have been detected in the CSF of patients with Lyme neuroborreliosis[42,43] as well as in the rhesus model.[44] *B. burgdorferi* has been shown to induce IL-6 in rat glioma cells.[45] Our findings expand on these results and indicate that astrocytes are among the cells that are a source of the IL-6 produced in the CNS in response to a *B. burgdorferi* infection.

Previously we reported on the production of the cytokine TNF-α in primary cultures of rhesus monkey astrocytes when these cells were stimulated with lipidated outer surface protein A (L-OspA, 1.0 μg/ml) *in vitro*.[44] L-OspA is a major lipoprotein of *B. burgdorferi*. We had also found that primary cultures of rhesus monkey microglia can produce TNF-α in response to L-OspA.[46] We did not detect TNF-α in brain sections stimulated with live spirochetes by immunofluorescence staining. However, we did see a significant increase in TNF-α transcript in spirochete-stimulated tissues by microarray analysis (21.7-fold) as well as by real time PCR (7.43-fold). Rhesus TNF-α is readily detectable with the anti-human TNF-α antibodies used in this study, as shown previously with a rhesus macaque model of chronic gut inflammation in which the same antibodies were used.[37] Therefore, it was not because of lack of antibody cross-reactivity that we failed to observe TNF-α production in brain tissues. Rather, it is possible that there was a lag in the kinetics of translation of TNF-α transcript. Specific inhibitors of TNF-α translation have been described.[47]

IL-1β, a cytokine that plays a key role in mediating inflammation in the CNS,[48] was produced by microglia in spirochete-stimulated brain tissues. Many different cell types in the brain express the IL-1 receptor and respond to this cytokine by activating cell-type-specific signaling

pathways leading to distinct functional responses.[49] Neurons also express the IL-1 receptor, indicating that this cytokine can influence neuronal function directly.[50] There is evidence that IL-1β can cause synaptic inhibition[51] and suppress long-term potentiation, two neuronal processes which are thought to be involved in learning and memory.[52] IL-1β is also involved in microglia-mediated neurotoxicity.[53] An inflammatory cascade of events triggered by IL-1β causes the decline of mental fitness in Alzheimer's disease.[54] IL-1β-mediated neuronal dysfunction could similarly be a possible player in the pathogenesis of Lyme neuroborreliosis.

Spirochetes elicited both the up-regulation of IL-8 transcript in brain tissues and production of this chemokine by astrocytes and microglia. The elevated levels of IL-8 found in the CSF of patients with Lyme neuroborreliosis[22] could indeed be caused by the interaction of spirochetes with glial cells, and be an effector of the inflammatory lesions seen in this form of Lyme disease, and of the leukocyte pleocytosis that is characteristic of Lyme meningitis. We also demonstrated the presence of the B-cell chemokine CXCL13 in microglia. Increased presence of CXCL13 or its transcript has been described in association with *B. burgdorferi* infection both in nonhuman primates and in humans.[55–57] CXCL13 also is produced by monocytes in response to molecules with the Pam3Cys motif of bacterial lipoproteins[58]; the *B. burgdorferi* genome contains more than 150 open reading frames that could encode such molecules.[59,60] Finally, COX-2, which we detected both in astrocytes and microglia, has emerged as a major player in the inflammatory reactions in the brain.[39] COX-2 is expressed in apoptotic oligodendrocytes in chronic active demyelinating lesions of patients with multiple sclerosis.[61] Activation of COX-2 contributes to motor and cognitive dysfunction,[62] and has been implicated in mediating neuropathic pain.[63] Others have shown *B. burgdorferi* to stimulate production of COX-2 in murine microglia,[64] an observation that is in accordance with ours in the rhesus model.

In addition to mediators elicited in glial cells, we observed the presence of IL-1β, IL-8, and COX-2 in glut-1-positive endothelial cells in blood vessels in tissue slices incubated with spirochetes plus brefeldin A, but not in control tissues held in medium plus brefeldin A after 4 hours of incubation (data not shown). Inflammatory changes induced in the CNS blood vessels as a result of interaction with *B. burgdorferi* spirochetes could be major players in the development of vasculitis seen in patients with Lyme neuroborreliosis.[5–8]

Cytokines, chemokines, other immune mediators, as well as glial and neuronal apoptosis have been documented to play a major role in inflammatory neurodegenerative diseases such as Alzheimer's disease, AIDS dementia,[65] and Parkinson's disease[66] in humans, and in simian immunodeficiency virus encephalitis in nonhuman primates.[67,68] The results of our microarray analysis emphasizes the possible role of immune function-related gene products as well as that of apoptosis-regulating genes in contributing to the pathogenesis of Lyme neuroborreliosis. Our observation of both neuronal and oligodendrocyte apoptosis *in situ* in *ex vivo*-stimulated brain tissues as well as in our stereotaxic *in vivo* model further affirms this role. A recent report demonstrates that phagocytosis of *B. burgdorferi* potentiates innate immune activation and induces apoptosis in human monocytes; this phenomenon is accompanied by the production of cytokines such as TNF-α, IL-1β, and IL-6.[69] Other *in vitro* studies have shown that IL-1β promotes oligodendrocyte death through glutamate excitotoxicity.[70] Oligodendrocyte death could also result in impaired neuronal function because these glial cells are vital for maintaining the normal nerve conduction.[71] Further detailed studies to explore the role of the various immune mediators and mechanisms involved in inducing glial and neuronal death will help answer these questions, and further our understanding of the signaling pathways that contribute to the pathogenesis of Lyme neuroborreliosis.

The levels of apoptosis of both oligodendrocytes and neurons were more marked when quantified by the TUNEL assay as compared to when they were measured via activated caspase-3. This could be attributable to the fact that the active caspase-3 assay only detects cells that are in the early stages of apoptosis,[72] whereas the TUNEL assay detects all nuclei showing fragmented DNA.[73] Importantly, the results obtained by both assays point in the same direction, with the percent apoptosis as detected by the active caspase-3 assay being approximately a third of the percent apoptosis as measured by TUNEL. The fact that we were also able to observe significant apoptosis of oligodendrocytes in our *in vivo* model of animals that were sterotaxically inoculated with live *B. burgdorferi* further illustrates that *B. burgdorferi* spirochetes have the ability to elicit oligodendrocyte apoptosis and confirms the observations of both oligodendrocyte and neuronal apoptosis seen in our *ex vivo* model. The reduced levels of oligodendrocyte and neuronal apoptosis observed *in vivo* as compared to that seen in the *ex vivo* specimens may be attributable to the action of phagocytic cells that would not only affect spirochetal burdens but also diminish the number of residual apoptotic cells at any time after inoculation.[74]

The proinflammatory cytokines TNF-α, IL-1β, and IL-6 have been reported to mediate apoptotic cell death of neurons by signaling via the p38 MAP kinase pathway in neurodegenerative conditions.[75] We have reported earlier that proliferation and apoptosis of astrocytes are mediated by IL-6 and TNF-α, respectively, as induced by stimulation of glial cells with L-OspA. We also reported that the phosphorylation of mitogen-activated protein kinases Erk 1/2 and P38 was involved in these phenomena.[76] These signaling mechanisms could also be operative in the pathogenesis of Lyme neuroborreliosis.

The major symptoms of long-term Lyme neuroborreliosis of the CNS, namely fatigue and cognitive dysfunction, could be a consequence of impairment of glial and neuronal cell function and survival as a result of the direct interaction between these cells and *B. burgdorferi*, or with the mediators elicited by the spirochete. The studies reported herein have helped identify glial cells as sources of immune mediators, as well as document the presence of concomitant apoptosis of both oligodendrocytes and neurons in spirochete-exposed parenchymal

tissues. They provide proof of the concept that inflammation with concomitant apoptosis are major factors in the pathogenesis of Lyme neuroborreliosis.

Acknowledgments

We thank Peter Mottram and Drs. Andrea Bernardino and Xavier Avarez for technical help and advice, and Robin Rodriguez for help with the confocal microscope images.

References

1. Steere AC, Grodzicki RL, Kornblatt AN, Craft JE, Barbour AG, Burgdorfer W, Schmid GP, Johnson E, Malawista SE: The spirochetal etiology of Lyme disease. N Engl J Med 1983, 308:733–740
2. Piesman J: Dynamics of Borrelia burgdoferi transmission by Ixodes dammini ticks. J Infect Dis 1993, 167:1082–1085
3. Steere AC: Lyme disease. N Engl J Med 2001, 345:115–125
4. Gustaw K, Beltowska K, Studzinska MM: Neurological and psychological symptoms after severe acute neuroborreliosis. Ann Agric Environ Med 2001, 8:91–94
5. Jacobi C, Schwark C, Kress B, Hug A, Storch-Hagenlocher B, Schwaninger M: Subarachnoid hemorrhage due to Borrelia burgdorferi-associated vasculitis. Eur J Neurol 2006, 13:536–538
6. Chehrenama M, Zagardo MT, Koski CL: Subarachnoid hemorrhage in a patient with Lyme disease. Neurology 1997, 48:520–523
7. Schmitt AB, Küker W, Nacimiento W: Neuroborreliosis with extensive cerebral vasculitis and multiple cerebral infarcts. Nervenarzt 1999, 70:167–171
8. Seijo Martínez M, Grandes Ibáñez J, García-Monocó JC: Spontaneous brain hemorrhage associated with Lyme neuroborreliosis. Neurologia 2001, 16:43–45
9. Kohler J: Lyme borreliosis: a case of transverse myelitis with syrinx cavity. Neurology 1989, 39:1553–1554
10. Benach JL, Garcia-Monoco JC: Aspects of the pathogenesis of neuroborreliosis. Lyme Disease: Molecular and Immunological Approaches. Edited by Schutzer S. Cold Spring Harbor, Cold Spring Harbor Laboratory Press, 1992, pp. 1–10
11. Oksi J, Kalimo H, Marttila RJ, Marjamaki M, Sonninen P, Nikoskelainen J, Viljanen MK: Inflammatory brain changes in Lyme borreliosis. A report on three patients and review of literature. Brain 1996, 119:2143–2154
12. Dryden MS, O'Connell S, Samuel W, Iannotti F: Lyme myelitis mimicking neurological malignancy. Lancet 1996, 348:624
13. Benveniste EN: Inflammatory cytokines within the central nervous system: sources, functions, and mechanisms of action. Am J Physiol 1992, 263:C1–C5
14. Merrill JE, Benveniste EN: Cytokines in inflammatory brain lesions: helpful and harmful. TINS 1996, 19:331–338
15. Rothwell NJ, Hopkins SJ: Cytokines and nervous system II: actions and mechanisms of action. Trends Neurosci 1995, 18:130–136
16. Raivich G, Jones LL, Werner A, Bluthmann, Doetschmann T, Kreutzberg GW: Molecular signals for glial activation: pro- and anti-inflammatory cytokines in the injured brain. Acta Neurochir Suppl 1999, 73:21–30
17. Wang WZ, Fredrikson S, Sun JB, Link H: Lyme neuroborreliosis: evidence for persistent up-regulation of Borrelia burgorferi-reactive cells secreting interferon-gamma. Scand J Immunol 1995, 42:694–700
18. Ekerfelt C, Jarefors S, Tynngard N, Hedlund M, Sander B, Bergstrom S, Forsberg P, Ernerudh J: Phenotypes indicating cytolytic properties of Borrelia-specific interferon-γ secreting cells on chronic Lyme neuroborreliosis. J Neuroimmunol 2003, 145:115–126
19. Kondrusik M, Sweirzbinska R, Pancewicz S, Zajkowska J, Grygorczuk S, Hermanowska-Szpakowicz T: Evaluation of proinflammatory cytokine (TNF-alpha, IL-1beta, IL-6, IFN-gamma) concentrations in serum and cerebrospinal fluid of patients with neuroborreliosis. Neurol Neurochir Pol 2004, 38:265–270
20. Widhe M, Grusell M, Ekerfelt C, Vrethem M, Forsberg P, Ernerudh J: Cytokines in Lyme borreliosis: lack of early tumor necrosis factor-α and transforming growth factor-β1 responses are associated with chronic neuroborreliosis. Immunology 2002, 107:46–55
21. Rupprecht TA, Pfister HW, Angele B, Kastenbauer S, Wilske B, Koedel U: The chemokine CXCL13 (BLC): a putative diagnostic marker for neuroborreliosis. Neurology 2005, 65:448–450
22. Grygorczuk S, Pancewicz S, Zajkowska J, Kondrusik M, Swierzbinska R, Hermanowska-Szpakowicz T: Concentration of macrophage inflammatory proteins MIP-α and MIP-β and interleukin 8 (IL-8) in Lyme borreliosis. Infection 2004, 32:350–355
23. Grygorczuk S, Zajkowska J, Swierzbinska R, Pancewicz S, Kondrusik M, Hermanowska-Szpakowicz T: Concentration of interferon-inducible T cell chemoattractant and monocyte chemotactic protein-1 with Lyme borreliosis. Ann Acad Med Bialo 2005, 50:173–178
24. Lewczuk P, Reiber H, Korenke GC, Bollensen E, Dorta-Contreras AJ: Intrathecal release of sICAM-1 into CSF in neuroborreliosis increased brain-derived fraction. J Neuroimmunol 2000, 103:93–96
25. Philipp MT, Aydintug MK, Bohm Jr RP, Cogswell FB, Dennis VA, Lanners HN, Lowrie Jr RC, Roberts ED, Conway MD, Karacorlu M, Peyman GA, Gubler DJ, Johnson BJB, Piesman J, Gu Y: Early and early-disseminated phases of Lyme disease in the rhesus monkey: a model of infection in humans. Infect Immun 1993, 61:3047–3059
26. Roberts ED, Bohm Jr RP, Cogswell FB, Lanners HN, Lowrie Jr RC, Povinelli L, Piesman J, Philipp MT: Chronic Lyme disease in the rhesus monkey. Lab Invest 1995, 72:146–160
27. Pachner AR, Delaney E, O'Neil T, Major E: Inoculation of non human primates with the N40 strain of Borrelia burgdorferi leads to a model of Lyme neuroborreliosis faithful to the human disease. Neurology 1995, 45:165–172
28. England JD, Bohm Jr R, Roberts ED, Philipp MT: Mononeuropathy multiplex in rhesus monkeys with chronic Lyme disease. Ann Neurol 1997, 41:375–384
29. Roberts ED, Bohm Jr RP, Lowrie Jr RC, Habicht G, Katona L, Piesman J, Philipp MT: Pathogenesis of Lyme neuroborreliosis in the rhesus monkey: the early disseminated and chronic phases of disease in the peripheral nervous system. J Infect Dis 1998, 178:722–732
30. Cadavid D, O'Neil T, Schaefer H, Pachner AR: Localization of Borrelia burgdorferi in the nervous system and other organs in a nonhuman primate model of Lyme disease. Lab Invest 2000, 80:1043–1054
31. Pachner AR: The rhesus model of Lyme neuroborreliosis. Immunol Rev 2001, 183:186–204
32. Bai Y, Narayan K, Dail D, Sondey M, Hodzic E, Barthold SW, Pachner AR, Cadavid D: Spinal cord involvement in the nonhuman primate model of Lyme disease. Lab Invest 2004, 84:160–172
33. Haber SN: The primate basal ganglia: a parallel and integrative networks. J Chem Neuroanat 2003, 26:317–330
34. Jackson CL: Brefeldin A revealing fundamental principles governing membrane dynamics and protein transport. Subcell Biochem 2000, 34:233–272
35. Ramamoorthy R, McClain NA, Gautum A, Scholl-Meeker D: Expression of the bmpB gene of Borelia burgdorferi is modulated by two distinct transcription termination events. J Bacteriol 2005, 187:2592–2600
36. Kaushal D, Naeve CW: Analyzing and visualizing expression data with Spotfire. Current Protocols in Bioinformatics. Edited by Baxevanis A. Hoboken, John Wiley and Sons Inc. 2004, pp 7.9.1–7.9.25
37. Ramesh G, Alvarez X, Borda JT, Aye PP, Lackner AA, Sestak K: Visualizing cytokine-secreting cells in situ in the rhesus macaque model of chronic gut inflammation. Clin Diag Lab Immunol 2005, 12:192–197
38. Schmidt-Kastner R, Szymas J: Immunohistochemistry of glial fibrillary acid protein, vimentin and S-100 protein for study of astrocytes in hippocampus of rat. J Chem Neuroanat 1990, 3:179–192
39. Minghetti L: Cyclooxygenase-2 (COX-2) in inflammatory and degenerative brain diseases. J Neuropathol Exp Neurol 2004, 63:901–910
40. Pachner AR, Amemiya K, Delaney E, O'Neil T, Hughes CAN, Zhang WF: Interleukin-6 is expressed at high levels in the CNS in Lyme neuroborreliosis. Neurology 1997, 49:147–152
41. Chiang CS, Stalder A, Campbell IL: Reactive gliosis as a consequence of interleukin 6 expression in the brain: studies in transgenic mice. Dev Neurosci 1994, 16:212–221
42. Dotevall L, Hagberg L, Karlsson JL, Rosengren LE: Astroglial and neuronal proteins in cerebrospinal fluid as markers of CNS involvement in Lyme neuroborreliosis. Eur J Neurol 1999, 6:169–178

43. Dotevall L, Rosengren LE, Hagberg L: Increased cerebrospinal fluid levels of glial fibrillary acidic protein (GFAP) in Lyme neuroborreliosis. Infection 1996, 24:125–129
44. Ramesh G, Alvarez AL, Roberts ED, Dennis VA, Lasater BL, Alvarez X, Philipp MT: Pathogenesis of Lyme neuroborreliosis: Borrelia burgdorferi lipoproteins induce both proliferation and apoptosis in rhesus monkey astrocytes. Eur J Immunol 2003, 33:2539–2550
45. Habicht GS, Katona LI, Benach JL: Cytokines and the pathogenesis of neuroborreliosis: Borrelia burgdorferi induces glioma cells to secrete interleukin-6. J Infect Dis 1991, 164:568–574
46. Ramesh G: An in vitro model of the interaction of bacterial lipoproteins with the central nervous system (Ph.D. thesis). [New Orleans (LA)]Tulane University
47. Piecyk M, Wax S, Beck AR, Kedersha N, Gupta M, Maritim B, Chen S, Gueydan C, Kruys V, Streuli M, Anderson P: TIA-1 is a translational silencer that selectively regulates the expression of TNF-alpha. EMBO J 2000, 19:4154–4163
48. Friedman WJ: Interactions of interleukin-1 with neurotropic factors in the central nervous system: beneficial or detrimental? Mol Neurobiol 2005, 32:133–144
49. Srinivasan D, Yen JH, Joseph DJ, Friedman W: Cell type-specific interleukin-1beta signaling in the CNS. J Neurosci 2004, 24:6482–6488
50. Friedman WJ: Cytokines regulate expression of the type 1 interleukin-1 receptor in rat hippocampal neurons and glia. Exp Neurol 2001, 168:23–31
51. Zeise ML, Madamba S, Siggins GR: Interleukin-1β increases synaptic inhibition in rat hippocampal pyramidal neurons in vitro. Regul Pept 1992, 39:1–7
52. Katsuki H, Nakai S, Hirai Y, Akaji K, Kiso Y, Satoh M: Interleukin-1β inhibits long-term potentiation in the CA3 region of mouse hippocampal slices. Eur J Pharmacol 1990, 181:323–326
53. Ma XC, Gottschall PE, Chen LT, Wiranowska M, Phelphs CP: Role and mechanisms of interleukin-1 in the modulation of neurotoxicity. Neuroimmunomodulation 2002–2003, 10:199–207
54. Griffin WS: Inflammation and neurodegenerative diseases. Am J Clin Nutr 2006, 83:470S–474S
55. Pachner AR, Dail D, Narayan K, Dutta K, Cadavid D: Increased expression of B-lymphocyte chemoattractant, but not pro-inflammatory cytokines, in muscle tissue in rhesus chronic Lyme borreliosis. Cytokine 2002, 19:297–307
56. Narayan K, Dail D, Li L, Cadavid D, Amrute S, Fitzgerald-Bocaesly P, Pachner AR: The nervous system as ectopic germinal center: CXCL13 and IgG in Lyme neuroborreliosis. Ann Neurol 2005, 57:813–823
57. Cadavid D: The mammalian host response to borrelia infection. Wien Klin Wochenschr 2006, 18:653–658
58. Rupprecht TA, Kirschning CJ, Popp B, Kastenbauer S, Fingerle V, Pfister HW, Koedel U: Borrelia garinii induces CXCL13 production in human monocytes through Toll-like receptor 2. Infect Immun 2007, 75:4351–4356
59. Fraser CM, Casjens S, Huang WM, Sutton GG, Clayton R, Lathigra R, White O, Ketchum KA, Dodson R, Hickey EK, Gwinn M, Dougherty B, Tomb JF, Fleischmann RD, Richardson D, Peterson J, Kerlavage AR, Quackenbush J, Salzberg S, Hanson M, van Vugt R, Palmer N, Adams MD, Gocayne J, Weidman J, Utterback T, Watthey L, McDonald L, Artiach P, Bowman C, Garland S, Fuji C, Cotton MD, Horst K, Roberts K, Hatch B, Smith HO, Venter JC: Genomic sequence of a Lyme disease spirochaete, Borrelia burgdorferi. Nature 1997, 390:580–586
60. Casjens S, Palmer N, van Vugt R, Huang WM, Stevenson B, Rosa P, Lathigra R, Sutton G, Peterson J, Dodson RJ, Haft D, Hickey E, Gwinn M, White O, Fraser CM: A bacterial genome in flux: the twelve linear and nine circular extrachromosomal DNAs in an infectious isolate of the Lyme disease spirochete Borrelia burgdorferi. Mol Microbiol 2000, 35:490–516
61. Carlson NG, Hill KE, Tsunoda I, Fujinami RS, Rose JW: The pathogenic role for COX-2 in apoptotic oligodendrocytes in virus induced demyelinating disease: implications for multiple sclerosis. J Neuroimmunol 2006, 174:21–31
62. Cernak I, O'Connor C, Vink R: Activation of cyclooxygenase-2 contributes to motor and cognitive dysfunction following diffuse traumatic brain injury in rats. Clin Exp Pharmacol Physiol 2001, 28:922–925
63. Ma W, Quirion R: Up-regulation of interleukin-6 induced by prostaglandin E from invading macrophages following nerve injury: an in vivo and in vitro study. J Neurochem 2005, 93:664–673
64. Rasley A, Anguita J, Marriot I: Borrelia burgdorferi induces inflammatory mediator production of murine microglia. J Neuroimmunol 2002, 130:22–31
65. Dickson DW, Lee SC, Mattiace LA, Yen SC, Brosnan C: Microglia and cytokines in neurological disease, with special reference to AIDS and Alzheimer's disease. Glia 1993, 7:75–83
66. Nagatsu T, Sawada M: Inflammatory process in Parkinson's disease: role for cytokines. Curr Pharm Des 2005, 11:999–1016
67. Orandle MT, MacLean AG, Sasseville VG, Alvarez X, Lackner AA: Enhanced expression of proinflammatory cytokines in the central nervous system is associated with neuroinvasion by simian immunodeficiency virus and the development of encephalitis. J Virol 2002, 76:5797–5802
68. Adamson DC, Dawson TM, Zink MC, Clements JE, Dawson VL: Neurovirulent simian immunodeficiency virus infection induces neuronal, endothelial and glial apoptosis. Mol Med 1996, 2:417–428
69. Cruz AR, Moore MW, La Vake CJ, Eggers CH, Salazar JC, Radolf JD: Phagocytosis of B. burgdorferi potentiates innate immune activation and induces apoptosis in human monocytes. Infect Immun 2008, 76:56–70
70. Takahashi JL, Giuliani F, Powe C, Imai Y, Young VW: Interleukin-beta promotes oligodendrocyte death through glutamate excitotoxicity. Ann Neurol 2003, 53:588–595
71. Compston A Zajicek J, Sussman J, Webb A, Hall G, Muir D, Shaw C, Wood A, Scolding N: Glial lineages and myelination in the central nervous system. J Anat 1997, 190:161–200
72. Namura S, Zhu J, Fink K, Endres M, Srinivasan A, Tomaselli KJ, Yuan J, Moskowitz MA: Activation and cleavage of caspase-3 in apoptosis induced by experimental cerebral ischemia. J Neurosci 1998, 18:3659–3668
73. de Torres C, Munell F, Ferrer I, Reventos J, Macaya A: Identification of necrotic cell death by the TUNEL assay in the hypoxic ischemic neonatal rat brain. Neurosci Lett 1997, 230:1–4
74. Maderna P, Godson C: Phagocytosis of apoptotic cells and resolution of inflammation. Biochem Biophys Acta 2003, 1639:141–151
75. Chaparro-Huerta V, Rivera-Cervantes MC, Flores-Soto ME, Gomez-Pinedo U, Beas-Zarate C: Proinflammatory cytokines and apoptosis following glutamate-induced excitotoxicity mediated by p38 MAPK in the hippocampus of neonatal rats. J Neuroimmunol 2005, 165:53–62
76. Ramesh G, Philipp MT: Pathogenesis of Lyme neuroborreliosis: mitogen-activated protein kinases Erk1, Erk2, and p38 in the response of astrocytes to Borrelia burgdorferi lipoproteins. Neurosci Lett 2005, 384:112–116